



**HAL**  
open science

## Detailed analysis of the isotopic composition of CO and characterization of the air masses arriving at Mount Sonnblick (Austrian Alps)

Valérie Gros, Maya Bräunlich, T. Röckmann, P. Jöckel, P. Bergamaschi, C. Brenninkmeijer, W. Rom, W. Kutschera, A. Kaiser, H. Scheel, et al.

► **To cite this version:**

Valérie Gros, Maya Bräunlich, T. Röckmann, P. Jöckel, P. Bergamaschi, et al.. Detailed analysis of the isotopic composition of CO and characterization of the air masses arriving at Mount Sonnblick (Austrian Alps). *Journal of Geophysical Research: Atmospheres*, 2001, 106 (D3), pp.3179-3193. 10.1029/2000JD900509 . hal-03117190

**HAL Id: hal-03117190**

**<https://hal.science/hal-03117190>**

Submitted on 21 Jan 2021

**HAL** is a multi-disciplinary open access archive for the deposit and dissemination of scientific research documents, whether they are published or not. The documents may come from teaching and research institutions in France or abroad, or from public or private research centers.

L'archive ouverte pluridisciplinaire **HAL**, est destinée au dépôt et à la diffusion de documents scientifiques de niveau recherche, publiés ou non, émanant des établissements d'enseignement et de recherche français ou étrangers, des laboratoires publics ou privés.

## Detailed analysis of the isotopic composition of CO and characterization of the air masses arriving at Mount Sonnblick (Austrian Alps)

Valérie Gros,<sup>1</sup> Maya Bräunlich,<sup>1</sup> T. Röckmann,<sup>1</sup> P. Jöckel,<sup>1</sup> P. Bergamaschi,<sup>1,2</sup> C.A.M. Brenninkmeijer,<sup>1</sup> W. Rom,<sup>3,4</sup> W. Kutschera,<sup>3</sup> A. Kaiser,<sup>5</sup> H. E. Scheel,<sup>6</sup> M. Mandl,<sup>7</sup> J. van der Plicht,<sup>8</sup> and G. Possnert<sup>9</sup>

**Abstract.** Air sampling for analysis of CO and its isotopic composition (<sup>13</sup>C, <sup>18</sup>O, and <sup>14</sup>C) has been performed at the alpine station Sonnblick (47°N, 13°E, 3106 m above sea level) since September 1996. A high degree of variability is observed, which is due to the wide variation in the origin of air masses sampled. On the basis of the CO and isotope results, a classification of the different samples is performed. Other data such as <sup>7</sup>Be, O<sub>3</sub>, relative humidity, and back trajectories are used to give additional information about the air mass origin. Background values, representative of the NH midlatitudes free troposphere, are observed about 50% of the time and are used to define seasonal cycles. CO and its isotopes show a minimum in summer and a maximum in winter with extreme values of 90 and 160 ppb for CO, -30 and -25 ‰ for δ<sup>13</sup>C, 0 and 8 ‰ for δ<sup>18</sup>O, and 8 and 20 molecules cm<sup>-3</sup> STP for <sup>14</sup>CO. CO and stable isotope data are compared with results from a three-dimensional model (TM2). Generally good agreement supports the CO, δ<sup>13</sup>CO, and δC<sup>18</sup>O source/sink distributions inferred by the model. According to model calculations, fossil fuel combustion contributes 35% in summer and 50% in winter of total CO for such a midlatitude location. Other categories of sampled air are “subtropical,” “polluted,” and “stratospheric” and are observed 24%, 18%, and 4% of the time. Corresponding signatures of CO and its isotopic variations are presented, and some specific events are discussed.

### 1. Introduction

As the main reaction partner of the hydroxyl radical (OH), carbon monoxide (CO) influences indirectly the abundance of several important atmospheric trace gases like methane or ozone [Intergovernmental Panel on Climate Change (IPCC), 1995]. The existing measurement networks allow one to derive the global background distribution of CO and to determine its seasonal cycle for the lower atmosphere [Novelli *et al.*, 1998, and references therein]. Furthermore, satellite data, now becoming available, will provide information about the vertical distribution [Edwards *et al.*, 1999; Bovensmann *et al.*, 1999]. Still, the quantification of the different CO sources and sinks will need a variety of approaches. Recent development of an inverse model for CO allows one to adjust source strengths according to observations [Bergamaschi *et al.*, 2000a]. The isotopic composition of CO imposes further

constraints on the global CO cycle and can improve our understanding of the more detailed processes, although at present inverse modeling still seems to require substantial improvements [Bergamaschi *et al.*, 2000b].

Isotopic analysis, although only applied on a limited scale, can help to study sources, whereas the isotope fractionation occurring during its reaction with OH gives information on the degree of removal in the atmosphere. For a recent review on CO isotopes, see Brenninkmeijer *et al.* [1999]. Here we only recall the isotopic signatures for the main CO sources, that is, fossil fuel combustion, oxidation of methane (CH<sub>4</sub>) and nonmethane hydrocarbons (NMHC), and biomass burning (Table 1). Other estimates are given by Bergamaschi *et al.* [2000b]. The main features are (1) the very depleted δ<sup>13</sup>C values for CO from methane oxidation, (2) the well defined δ<sup>18</sup>O signature for the fossil fuel combustion source, and (3) the considerable uncertainty of δ<sup>18</sup>O associated to the secondary sources of CO (oxidation of CH<sub>4</sub> and NMHC). Knowing the isotopic composition of the sources is necessary but not sufficient. One also has to know the fractionation occurring during CO sink processes, most importantly oxidation by OH. Kinetic isotope effects (KIEs) enrich the remaining CO in <sup>13</sup>C and deplete it in <sup>18</sup>O [Stevens and Wagner, 1989; Röckmann *et al.*, 1998].

Concerning <sup>14</sup>CO, this ultra trace gas can be considered to a large degree as independent of CO itself. Indeed, approximately ¾ of all <sup>14</sup>CO in the atmosphere is of direct cosmogenic origin; that is, <sup>14</sup>C is produced by the neutron-proton exchange reaction in nitrogen <sup>14</sup>N (n,p) <sup>14</sup>C, after which it is rapidly oxidized to <sup>14</sup>CO [MacKay *et al.*, 1963; Pandow *et al.*, 1960]. The remaining ¼ is referred to as “recycled” <sup>14</sup>C, and is of biogenic origin. For instance, the oxidation by OH of CH<sub>4</sub>, which is mainly biogenic and contains <sup>14</sup>C, produces <sup>14</sup>CO. The average abundance of <sup>14</sup>CO

<sup>1</sup>Air Chemistry Division, Max Planck Institute for Chemistry, Mainz, Germany.

<sup>2</sup>Now at Kirchzarten, Germany.

<sup>3</sup>Vienna Environmental Research Accelerator, Institute for Isotope Research and Nuclear Physics, University of Vienna, Vienna, Austria.

<sup>4</sup>Now at <sup>14</sup>C Dating Laboratory, Aarhus, Denmark.

<sup>5</sup>Central Institute for Meteorology and Geodynamics, Vienna, Austria.

<sup>6</sup>Fraunhofer Institute, Garmisch-Partenkirchen, Germany.

<sup>7</sup>Central Institute for Meteorology and Geodynamics, Salzburg, Austria.

<sup>8</sup>Centre for Isotope Research, University of Groningen, Netherlands.

<sup>9</sup>Ångström Laboratory, University of Uppsala, Uppsala, Sweden.

**Table 1.** Inferred and Measured Isotopic Composition for the Main Sources of CO

	$\delta^{13}\text{C}$ (‰) V-PDB	$\delta^{18}\text{O}$ (‰) V-SMOW
Fossil fuel combustion	-27.4 <sup>a</sup>	23.5 <sup>a,b</sup>
Biomass burning	-21.3 <sup>c</sup>	-16 <sup>c</sup>
	-24.5 <sup>d</sup>	-18 <sup>c</sup>
CH <sub>4</sub> oxidation	-52.6 <sup>f</sup>	0 <sup>e,g</sup>
		15 <sup>e</sup>
NMHC oxidation	-32 <sup>e</sup>	0 <sup>e,h</sup>
		15 <sup>e</sup>

<sup>a</sup> Stevens *et al.* [1972]<sup>b</sup> Brenninkmeijer [1993]<sup>c</sup> Conny *et al.* [1997]<sup>d</sup> Conny [1998]<sup>e</sup> Stevens and Wagner [1989]<sup>f</sup> Based on  $\delta^{13}\text{C}$  of CH<sub>4</sub>, -47.2‰ [Quay *et al.*, 1991] and on the fractionation in CH<sub>4</sub> + OH of 5.4‰ [Cantrell *et al.*, 1990], assuming quantitative conversion of CH<sub>4</sub> into CO.<sup>g</sup> Brenninkmeijer and Röckmann [1997]

in the troposphere is very low, in the range of 5 to 30 molecules cm<sup>-3</sup>. The total source of <sup>14</sup>CO being largely independent from human activities makes <sup>14</sup>CO an excellent tracer for investigating long-term changes in the atmosphere. However, <sup>14</sup>CO has the OH and soil sink in common with CO. It has been proposed that <sup>14</sup>CO may track changes in OH, but also differences in Stratosphere-Troposphere Exchange (STE) [Brenninkmeijer *et al.*, 1992; Jöckel *et al.*, 2000].

Over the last few years, data from an increasing number of stations, where air sampling for CO isotope measurements is performed, have allowed a first picture of CO isotopic changes and seasonal cycles to be drawn. Most of these stations are located at remote locations, often in marine environments, where the long distances from the main CO source areas allow background air to be sampled most of the time. Only few specific studies have been performed in continental areas [Volz *et al.*, 1981; Huff and Thiemens, 1998; Kato *et al.*, 1999; Tyler *et al.*, 1999; Mak and Kra, 1999; Kato *et al.*, 2000]. Measurements in continental areas are quite difficult to interpret because of the mixing of emissions from surrounding sources into the background air. The risk is that the recorded signal is partly local and therefore not representative on the regional/continental scale. This is especially critical for CO which is emitted by various technological sources. In contrast, <sup>14</sup>CO measurements, largely independent from anthropogenic emissions, can also be used at continental sites. The alpine station Sonnblick, located in the lower free troposphere, has the advantage of giving access to clean air as well as polluted air when the station is influenced by boundary layer air. The Alps are situated between areas of major pollution, in particular Munich and the Po Basin which affect the air masses arriving at Mount Sonnblick [Seibert *et al.*, 1998]. The objective of this paper is to analyze CO and its isotope variations for this continental station.

## 2. Experiments

### 2.1. Station

The Sonnblick Observatory is located in the Austrian Alps (47°03'N, 12°57'E) in a national park at the top of Mount Sonnblick (3106 m above sea level (asl)). The surrounding area consists of a glacier to the south and a very steep 500 m drop to

the north. The nearest town, Zell am See (10,000 inhabitants.), is 40 km to the north. The larger cities Salzburg (150,000) in the northeast and Klagenfurt (100,000) in the southeast are about 125 km away. The observatory is nearly free from local pollution sources. It was established in 1886, and some meteorological records go back over 100 years.

### 2.2. CO and Isotopes Measurements

Air sampling for the CO isotopes started at Mt. Sonnblick in September 1996. Usually, a sample was collected once every 2 weeks. This frequency has fluctuated due to the restricted access in case of bad weather. At times, duplicates were collected and on several occasions sampling was repeated over 1 or more days. One hundred five samples were collected and analyzed, of which 37 were duplicates or repeated samples. In the next sections the total number of samples refers to 68; duplicates and repeated samples are not counted in the statistics.

Air is collected, via a 10 m, ½ inch diameter PFA line, by a modified three-stage RIX oil-free piston compressor [Mak and Brenninkmeijer, 1994]. The sample is dried at the inlet (Drierite), and the overall contamination of the system is less than 1 ppb. In this paper we will use "ppb" to express molar fractions, nmole/mole. For a typical sample, 600 L of air are collected within 1 hour and compressed into aluminum cylinders of 5 L volume (Scott Marrin, California). Time elapsed between sampling and analysis is a few weeks, without significant change in CO concentration.

The method used for the isotope analysis is based on the quantitative conversion of CO to CO<sub>2</sub> [Brenninkmeijer, 1993; Röckmann, 1998; Brenninkmeijer *et al.*, 1999, 2000]. The first step involves the complete removal of CO<sub>2</sub>, N<sub>2</sub>O and other condensable gases by Russian doll traps at liquid nitrogen temperature. The next step consists of the quantitative conversion of CO to CO<sub>2</sub> by Schütze reagent (I<sub>2</sub>O<sub>5</sub> on acidified silica gel). The CO<sub>2</sub> formed is trapped, and the amount of CO-derived CO<sub>2</sub> is manometrically determined with an absolute uncertainty of routinely less than 2% and a relative error below 1%. Finally, the CO<sub>2</sub> sample is assayed on a dual inlet mass spectrometer for the determination of  $\delta^{13}\text{C}$  and  $\delta^{18}\text{O}$  with an uncertainty of less than 0.2‰ and 0.4‰, respectively. The  $\delta$  notation stands for  $\delta = (R_{\text{sa}}/R_{\text{st}} - 1)$  with R denoting the ratio considered (i.e., <sup>13</sup>C/<sup>12</sup>C or <sup>18</sup>O/<sup>16</sup>O) for a sample (sa) or a standard (st). The reference standards are Vienna-PeeDee Belemnite (V-PDB) and Vienna-Standard Mean Ocean Water (V-SMOW) for  $\delta^{13}\text{C}$  and  $\delta^{18}\text{O}$ , respectively.

For analysis of the <sup>14</sup>C content, the CO<sub>2</sub> is accurately diluted using a nearly <sup>14</sup>C free gas and then submitted for Accelerator Mass Spectrometry. The Vienna Environmental Research Accelerator (VERA) laboratory provided most of the <sup>14</sup>CO results reported here. Additional analyses were performed in the Ångström laboratory (University of Uppsala, Sweden) and in the Centre for Isotope Research (University of Groningen, Netherlands). The <sup>14</sup>CO is determined with an overall uncertainty of 2 to 3% [Rom *et al.*, 2000a].

To check the reproducibility of the measurement, at times a second air sample was collected within 4 hours. The differences measured between the two samples depend on the reproducibility of sampling, storage, and analysis. Ten pairs were sampled at Sonnblick, and standard deviations calculated from the repeats were 2.1 ppb for CO, 0.1‰ for  $\delta^{13}\text{C}$ , 0.3‰ for  $\delta^{18}\text{O}$ , and 0.2 molecules cm<sup>-3</sup> for <sup>14</sup>CO. These results confirm the good reproducibility of the measurements [cf. Rom *et al.*, 2000a]. Because the duplicates were all sampled during background

conditions, these data also prove the low variability of CO over periods of several hours during background conditions.

### 2.3. Other Measurements

On each air sample collected, mixing ratios of methane ( $\text{CH}_4$ ), carbon dioxide ( $\text{CO}_2$ ), nitrous oxide ( $\text{N}_2\text{O}$ ), and sulfur hexafluoride ( $\text{SF}_6$ ) were measured [Bergamaschi *et al.*, 2000c]. These gases can help to track the origin of the air masses.  $\text{SF}_6$  is entirely produced by human activities [Maiss *et al.*, 1996; Maiss and Brenninkmeijer, 1998] and is a good indicator of polluted air.

Among the other parameters available for Sonnblick, we are especially interested in indicators of stratospheric air; namely, beryllium 7 ( $^7\text{Be}$ ), ozone ( $\text{O}_3$ ), and relative humidity (RH). Beryllium 7 is a cosmogenic radionuclide with a radioactive decay half-life of 53.3 days. It is mainly produced in the stratosphere, and values higher than  $8 \text{ mBq m}^{-3}$  in the lower troposphere are generally indicative of a stratospheric influence [Stohl *et al.*, 2000, and references therein]. Daily filter samples were collected at Sonnblick by the Federal Institute for Food Control, Linz, Austria (W. Ringer, personal communication, 1999). Continuous measurements of  $\text{O}_3$  were performed by the "Umweltbundesamt," Vienna, Austria. Finally, the meteorological parameters temperature, RH, wind speed and direction, and air pressure were provided by the Central Institute for Meteorology and Geodynamics.

### 2.4. Back Trajectories

Back trajectories were calculated using two methods. The Central Institute for Meteorology and Geodynamics (Vienna, Austria) calculated 4-day back trajectories with the "EUROPAMODELL" of the Deutscher Wetter Dienst [Fay *et al.*, 1995]. Further, we used the HYSPLIT 4.0 (Hybrid Single-Particle Lagrangian Integrated Trajectory) program from the National Oceanic and Atmospheric Administration (NOAA) to calculate 10-day back trajectories [Draxler and Hess, 1997]. When calculating trajectories with both methods, we found a good agreement.

### 2.5. 3-D Modeling

Data for CO,  $\delta^{13}\text{C}$ , and  $\delta^{18}\text{O}$  are compared to the output of a three-dimensional atmospheric transport model TM2 described by Bergamaschi *et al.* [2000a, 2000b]. The horizontal resolution of the model is  $8^\circ$  latitude by  $10^\circ$  longitude. The strengths of the sources used in the model were calculated using an inversion technique. The model uses the "a priori" contribution of each source and determines the corresponding distribution of CO. By comparing calculated and observed distributions, the inversion determines the "a posteriori" contribution of each source. Bergamaschi *et al.* [2000a, 2000b] have used different scenarios in order to test the sensitivity of the model to several parameters. We have extracted the model data of the base scenario S2 for the Sonnblick station.

## 3. Results and Discussion

The measurements are presented in Figure 1 for the whole period (September 1996 to August 1999). The striking feature is, except for  $\delta^{13}\text{C}$ , the large scatter observed. The first task is to identify the main processes causing this high degree of variability. Sonnblick's location at more than 3000 m altitude, well above the boundary layer height, should see background tropospheric air at most times. However, the scatter observed indicates air masses of

quite different origin. After a careful examination of CO and isotopes measurements and of the available supplementary data, we classified all samples in four different categories:

Background air is free tropospheric air originating from the mid-latitudes of the Northern Hemisphere. It is difficult to construct rigid criteria for selecting air samples representing background conditions. Typically, background air represents air that had not been recently affected by one of the following three sources (subtropics, pollution, stratosphere). The backward trajectories corresponding to the selected background samples supported this classification, indicating an origin of the air masses in the latitude range  $35^\circ\text{N}$ -  $65^\circ\text{N}$ .

Subtropical air is air from low latitudes. These samples were characterized by low values of  $^{14}\text{CO}$ , CO, and  $\delta^{18}\text{O}$ .

Polluted air is air partly originating from the boundary layer. These samples were identified based on their simultaneously elevated CO and  $\delta^{18}\text{O}$  values.

Stratospheric air is air that had a recent contact with the stratosphere or air which was affected by a stratospheric intrusion. The corresponding signature is a concomitant elevation of  $^{14}\text{CO}$ ,  $^7\text{Be}$ , and  $\text{O}_3$  values combined with low RH.

One sample (August 22, 1997) was excluded from the study due to local contamination (high CO and high  $\delta^{18}\text{O}$  corresponding to a diesel generator start at the station [Rom *et al.*, 2000b]). Finally, four samples showing unexpectedly high values of  $^{14}\text{CO}$  without concomitant elevation of  $^7\text{Be}$  and  $\text{O}_3$  and therefore a priori not linked to stratospheric influence were not classified in the four previous categories. One of them, collected on November 12, 1998, was likely due to human error. The three others are associated with quite high CO and high  $\delta^{18}\text{O}$  suggesting polluted air from the boundary layer. We do not explain the high  $^{14}\text{CO}$  associated to these samples; however, one cannot rule out the possible effects of nuclear power plant emissions. Nevertheless, very little information is available concerning emissions of  $^{14}\text{CO}$  by the nuclear power industry.

## 4. Background Air

### 4.1. Seasonal Variations

The results of the background data, which represent nearly 50% of the whole data set, are given in Figure 1 along with a curve fitting and results from the TM2 model [Bergamaschi *et al.*, 2000a, 2000b]. The curve fitting was calculated by applying a low-pass convolution filter [Jöckel, 2000]. Sensitivity tests were performed to determine the adequate filter time window using 1, 2 or 4 weeks. We selected a 2-week time window; nevertheless, one should keep in mind the uncertainty associated with the minimum and the maximum of the curve fitting, due to the few corresponding data points. We estimated these uncertainties by calculating the difference observed for the maximum and minimum points for the different time window calculations. The uncertainties are  $\pm 5 \text{ ppb}$  for CO,  $\pm 0.5 \text{ ‰}$  for  $\delta^{18}\text{O}$ ,  $\pm 0.3 \text{ ‰}$  for  $\delta^{13}\text{C}$ , and  $\pm 0.6 \text{ molecules cm}^{-3}$  for  $^{14}\text{CO}$ . As indicated in Figure 1, three data points have not been considered for the curve fitting of CO and  $\delta^{18}\text{O}$ , and they will be discussed separately.

The seasonal cycle of the background CO mixing ratio observed at Sonnblick has a minimum in summer of about 90 ppb and a maximum in late winter of about 160 ppb. This seasonal variation is mainly controlled by the seasonality of its main sink, that is, OH oxidation, OH concentrations being maximum in summertime. No significant interannual variation can be discerned from the small number of data points.

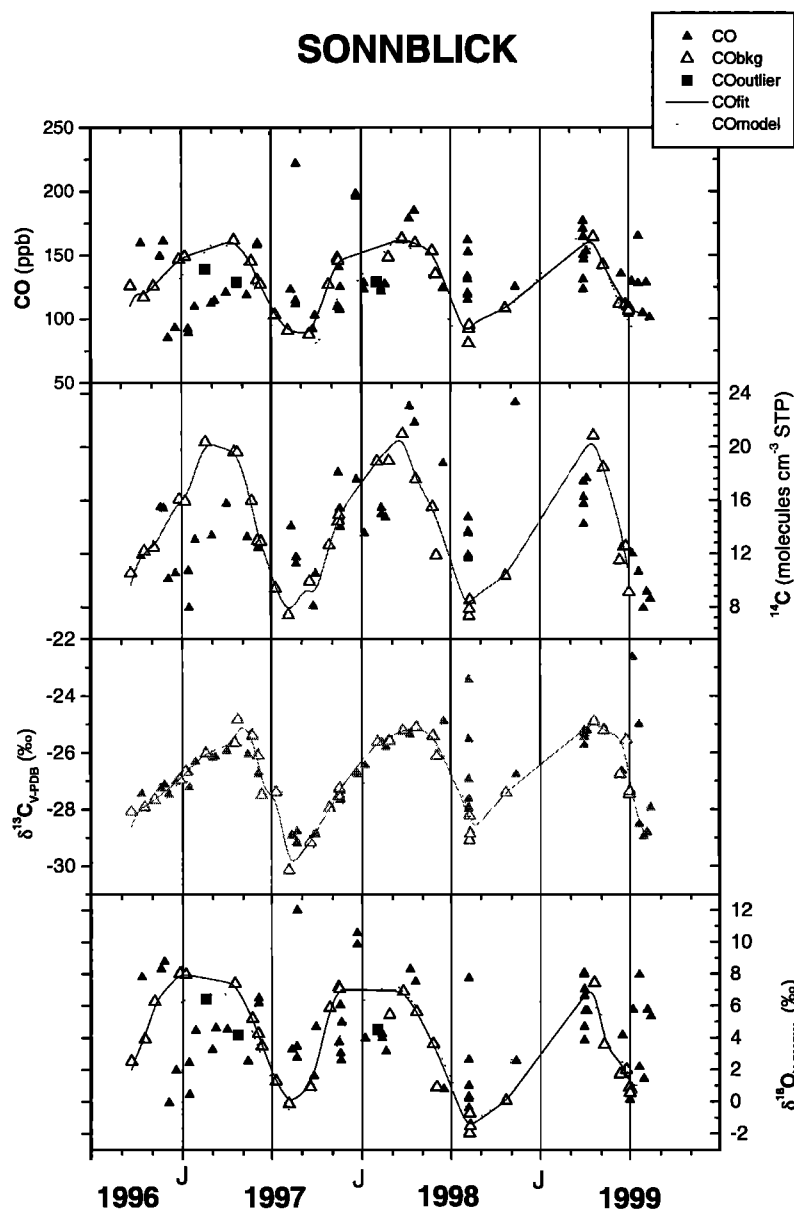


**Figure 1.** Complete data set of CO and isotopes ( $^{14}\text{C}$ ,  $\delta^{13}\text{C}$ ,  $\delta^{18}\text{O}$ ) obtained at Sonnblick between September 1996 and August 1999. The label J indicates January 1 of each year. Open triangles stand for background data; solid squares represent three outliers which are not taken into account in the curve fitting of CO and  $\delta^{18}\text{O}$  (see text). Curve fittings (solid line) and results of the 3-D model TM2 (dotted line) are also represented. Solid triangles stand for nonbackground data.

As the model calculations from *Bergamaschi et al.* [2000a] are based on meteorological data from 1987 and CO observations from 1993 to 1995, they can only give a typical seasonal cycle. Results of the TM2 model vary from 75 ppb in summer to 165 ppb in winter. These values are slightly lower than the observations for summer and fall, but actually the agreement with the observations is quite good, especially when considering the coarse grid of the model as well as the uncertainties associated with the curve fitting. We also want to point out here that we compare two curves using different criteria because the model calculations take into account all kinds of air masses, whereas our background signal excludes all data affected by pollution, subtropics, and stratosphere. However, we suggest that our background curve is, within the uncertainty, a good representation

of the annual mean signal and therefore that it is adequate to compare it with model outputs. This assumption is consistent with the fact that almost the same number of subtropical and polluted events are observed (see section 2) and that their opposite effects on CO and isotope compensate, at least partly, each other.

The contributions of the different CO sources derived from the model results are presented in Figure 2. Fossil fuel combustion contributes about 35% in summer and 50% in winter to the total CO. In contrast, the contribution from methane oxidation peaks in summer (30%) and decreases in winter (15%). The nonmethane hydrocarbon oxidation source has a constant contribution of 25 to 30% over the year. The contribution from the biomass burning source, 8% in yearly average, is at a maximum between April and June. We compared this partitioning of CO sources with those

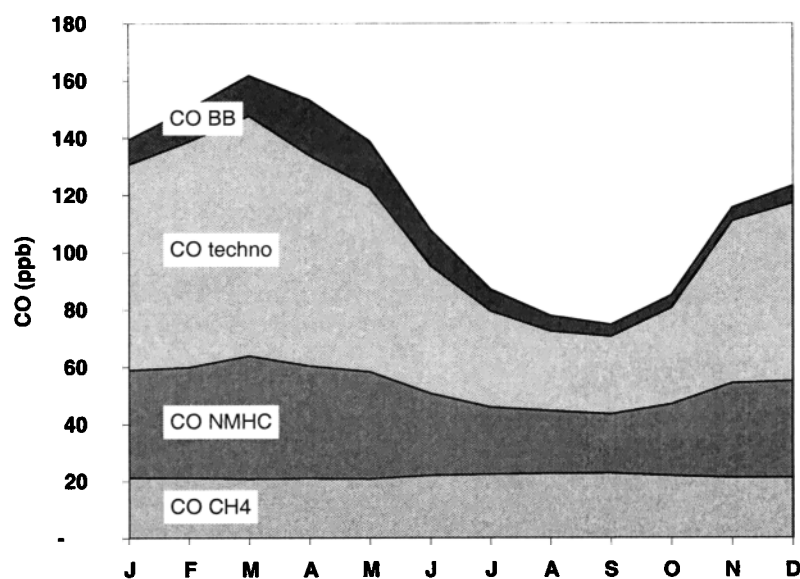


Figure 2. Contributions of CO sources to total CO according to TM2 model results.

from different stations of the Northern Hemisphere (Alert, 82°N; Cold Bay, 55°N; Tenerife, 28°N; Barbados, 13°N; Christmas Island, 2°N) [Bergamaschi *et al.*, 2000a]. We note that the fossil fuel contribution is almost the same (35% on annual average) for the mid and high latitudes of the Northern Hemisphere, whereas this contribution is significantly lower in the tropics (25% and 15% on annual average for Barbados and Christmas Island, respectively).

The CO mixing ratios may be compared with results from the Zugspitze, another alpine station (47°N, 11°E, 2962 m asl, at 150 km distance from Sonnblick), where CO has been monitored since 1990 [Scheel *et al.*, 1998]. Despite the high degree of variability observed at the Zugspitze, there is a good agreement. A comparison between Sonnblick and Zugspitze is given in Figure 3

for 1997. Except for the sample collected on April 24, which is one of the three outliers to be discussed later, we note the excellent agreement between the two data sets. Thus specific events of low CO (corresponding to clean air from southern latitudes, see section 2a) or high CO (corresponding to polluted air from the boundary layer, see section 2b) are captured nearly simultaneously by the two stations; large-scale advection yields similar trace gas variations at the two high-altitude alpine sites.

For Mace Head (Ireland, 53°N), Derwent *et al.* [1998] have determined a seasonal cycle of CO representative of “Northern Hemisphere Mid Latitudes Background (NHMLB)” with a maximum in April of 160 ppb and a minimum in July-August of 90 ppb. These variations are in good agreement with the background CO at Sonnblick, although the two stations have

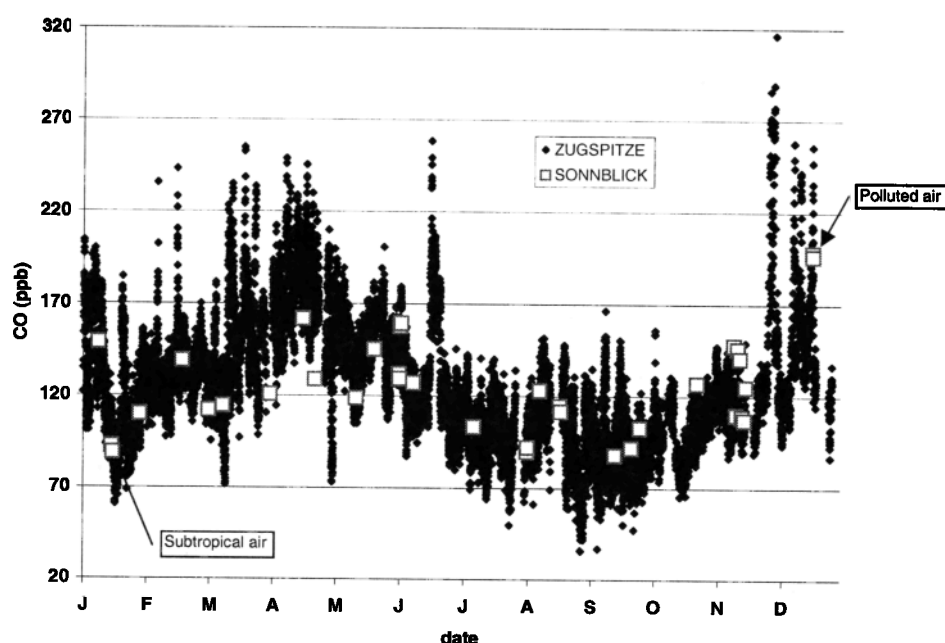


Figure 3. CO measurements at Sonnblick and Zugspitze in 1997. During the pollution event observed on December 4 at Zugspitze, CO peaked at 400 ppb and is not shown here.

different characteristics (boundary layer of the western extreme of Europe for Mace Head versus lower free troposphere of central Europe for Sonnblick). The similar signals derived from these two sites confirm the assumption that our "background" cycle observed at Sonnblick is reasonably representative of the midlatitudes of the NH troposphere.

The NOAA/CMDL sampling site in Hungary (47°N, 16°E, 240 m asl) is one of the few locations in continental Europe where CO is measured in the boundary layer. Despite a high degree of variability in the measurements, a significant seasonal cycle can be discerned with lowest values of 100 ppb observed in summer and up to 500 ppb found in winter [Novelli *et al.*, 1998]. The amplitude observed, about 3 times larger than the background signal derived at Sonnblick, reflects the effects of local and regional pollution.

The shape of the  $\delta^{18}\text{O}$  seasonal cycle is similar to that of the CO cycle, with a maximum of 7 to 8 ‰ in winter and a minimum of -2 to 0 ‰ in summer. This cycle is mainly controlled by two factors, one of which is the OH seasonality. The  $^{18}\text{O}$  kinetic isotope effect of approximately -10 ‰ leads to a preferential removal of the  $\text{C}^{18}\text{O}$  isotopomer inducing a  $\delta^{18}\text{O}$  minimum near the maximum in OH. The effect is enhanced by the winter maximum in the relative contribution from the fossil fuel combustion source, which is a source with a  $\delta^{18}\text{O}$  value of +23.5 ‰ [Stevens *et al.*, 1972; Brenninkmeijer, 1993] and the main CO source in the midlatitudes of the NH [Bergamaschi *et al.*, 2000a].

Comparing the  $\delta^{18}\text{O}$  data to model results shows generally good agreement (Figure 1), with model results varying from -1‰ in summer to 7 ‰ in winter. Model calculations are slightly lower than the observations between September and March. As modeled CO mixing ratios are also lower than the observations (see above), this suggests that the technological source is slightly underestimated in the model for the fall period.

The measured  $\delta^{13}\text{C}$  signal does not show much scatter, and the annual average is  $-27.1 \pm 1.5$  ‰. Two samples, with a  $\delta^{13}\text{C}$  value of -22‰, are considered as outliers and no explanation can be given. Like CO and  $\delta^{18}\text{O}$ , the  $\delta^{13}\text{C}$  seasonal cycle has also a minimum (-30‰ to -29‰) in summer, but here the maximum (around -25 ‰) is slightly delayed toward spring. This shift of about 1 month is due to the fact that the major sink and source effects are not in phase. Concerning the sources, the most significant effect comes from the methane oxidation source which is very depleted in  $\delta^{13}\text{C}$  (presumably -52‰ [Brenninkmeijer, 1993]) and thus leads to lower  $\delta^{13}\text{C}$  in summer. In contrast, the  $^{13}\text{C}$  KIE in the sink reaction (2 ‰ at 500 hPa and 5 ‰ at 1000 hPa) causes an increase in  $^{13}\text{CO}$  in spring and summer [Smit *et al.*, 1982; Stevens and Wagner, 1989]. Thus in spring, when fossil fuel combustion sources are still important and when OH begins to increase,  $\delta^{13}\text{C}$  increases and reaches its maximum. In summer, despite persistent high levels of OH, the source effect, linked to the very depleted methane oxidation source, predominates, and  $\delta^{13}\text{C}$  reaches a minimum [Brenninkmeijer, 1993].

Modeled  $\delta^{13}\text{C}$  presents a seasonal cycle with a maximum in May (-25.5 ‰) and a minimum in September (-29.5‰), in good agreement with the observed cycle. The model captures well the shift of the maximum from winter to spring; however, it also slightly shifts the minimum from August to September, which is not observed in the measurements. The highest discrepancy between model and data is observed between January and April, when model calculations are lower than the observations by 1.5‰.

Carbon monoxide 14 displays a seasonal cycle similar to CO with a winter maximum of 20 molecules  $\text{cm}^{-3}$  and a summer minimum of 8 molecules  $\text{cm}^{-3}$ . On the basis of the CO source

contributions obtained by the model, we can calculate the contribution of "recycled"  $^{14}\text{CO}$ . Knowing that sources emitting recycled  $^{14}\text{CO}$ , that is, hydrocarbon oxidation and biomass burning, have the equivalent of 0.038  $^{14}\text{CO}$  molecules  $\text{cm}^{-3}$  per ppb CO [Brenninkmeijer, 1993], we calculate that recycled CO contributes about 28% of total  $^{14}\text{CO}$  in summer and only 15% in winter.

As the main source of  $^{14}\text{CO}$  is cosmogenic and hardly exhibits a seasonal cycle, the observed seasonal variation is mostly controlled by the OH sink [Volz *et al.*, 1981]. The existing observations showed that  $^{14}\text{CO}$  has a strong latitudinal gradient in the NH, with values increasing with increasing latitudes. The range of concentrations measured at different stations is: 10-25 molecules  $\text{cm}^{-3}$  at Spitzbergen, 79°N (T. Röckmann *et al.*, manuscript in preparation, 2000), 7-17 molecules  $\text{cm}^{-3}$  at Izaña, 28°N (M. Bräunlich *et al.*, manuscript in preparation, 2000), 5-10 molecules  $\text{cm}^{-3}$  at Barbados, 13°N [Mak and Southon, 1998]. The results of 8-20 molecules  $\text{cm}^{-3}$  observed at Sonnblick, 47°N, are in the expected range. This gradient is due to the OH distribution, with higher values in the tropics than in the polar regions, and due to the latitudinal effect of the source as  $^{14}\text{CO}$  production rates also depend on latitude, with highest values north of 60°N [Lingenfelter, 1963; Jöckel *et al.*, 1999].

#### 4.2. Interannual Variations

$\delta^{18}\text{O}$  and  $^{14}\text{CO}$  are plotted against CO in Figures 4a and 4b for 1997 and 1998 (1996 and 1999 are incomplete and therefore not presented), including model results for  $\text{C}^{18}\text{O}$ . In Figure 4a we note the following:

1. For each year we observe an ellipsoid-shape curve which is well reproduced by the model. It shows that the transition from winter to summer and from summer to winter are slightly different. For a given value of CO,  $\delta^{18}\text{O}$  is higher by 2‰ in fall than in spring. The structure observed here is due to a small phase shift of the seasonality of CO and  $\text{C}^{18}\text{O}$  sources and sinks.

2. For a given value of CO,  $\delta^{18}\text{O}$  is lower by 1‰ in 1998. If this difference were due to a sink effect, this would imply significantly higher concentrations of OH in 1998. A calculation with a box model, assuming a OH concentration of  $10^6$  molecules  $\text{m}^{-3}$ , shows that the increase in OH should be about 15% to explain a 1‰ decrease of  $\delta^{18}\text{O}$ . However, as interannual variations in OH concentrations are expected to be only about 0.5 ‰ [Krol *et al.*, 1998] and as no major atmospheric changes have been reported either, this hypothesis is not realistic. Thus a change in CO sources must have occurred between these 2 years.

Lower  $\delta^{18}\text{O}$  for an identical CO value, or conversely higher CO for an identical  $\delta^{18}\text{O}$  value, points to different contributions of the CO sources for the years considered. Among the different sources of CO, biomass burning is the one most likely to have led to this change of CO composition. Indeed, this source, which is known to significantly fluctuate from one year to another [Cooke *et al.*, 1996], has been reported to be especially intense in the tropics in late 1997-early 1998 [Levine, 1999]. As biomass burning is a source moderately enriched in  $\text{C}^{18}\text{O}$  and as Sonnblick is located far away from the source regions, the long time of transport/mixing leads to the removal of proportionally more  $\text{C}^{18}\text{O}$  than  $\text{C}^{16}\text{O}$  (for a reduction to 1/e, a 10‰ depletion occurs). This assumption is consistent with the observations at Izaña (28°N) which present the same feature of lower  $\delta^{18}\text{O}$  (for a same CO value) in 1998 compared to 1997 (M. Bräunlich *et al.*, manuscript in preparation, 2000).

In Figure 4b,  $^{14}\text{CO}$  and CO have been normalized to compare their relative seasonal change. The near linear relationship

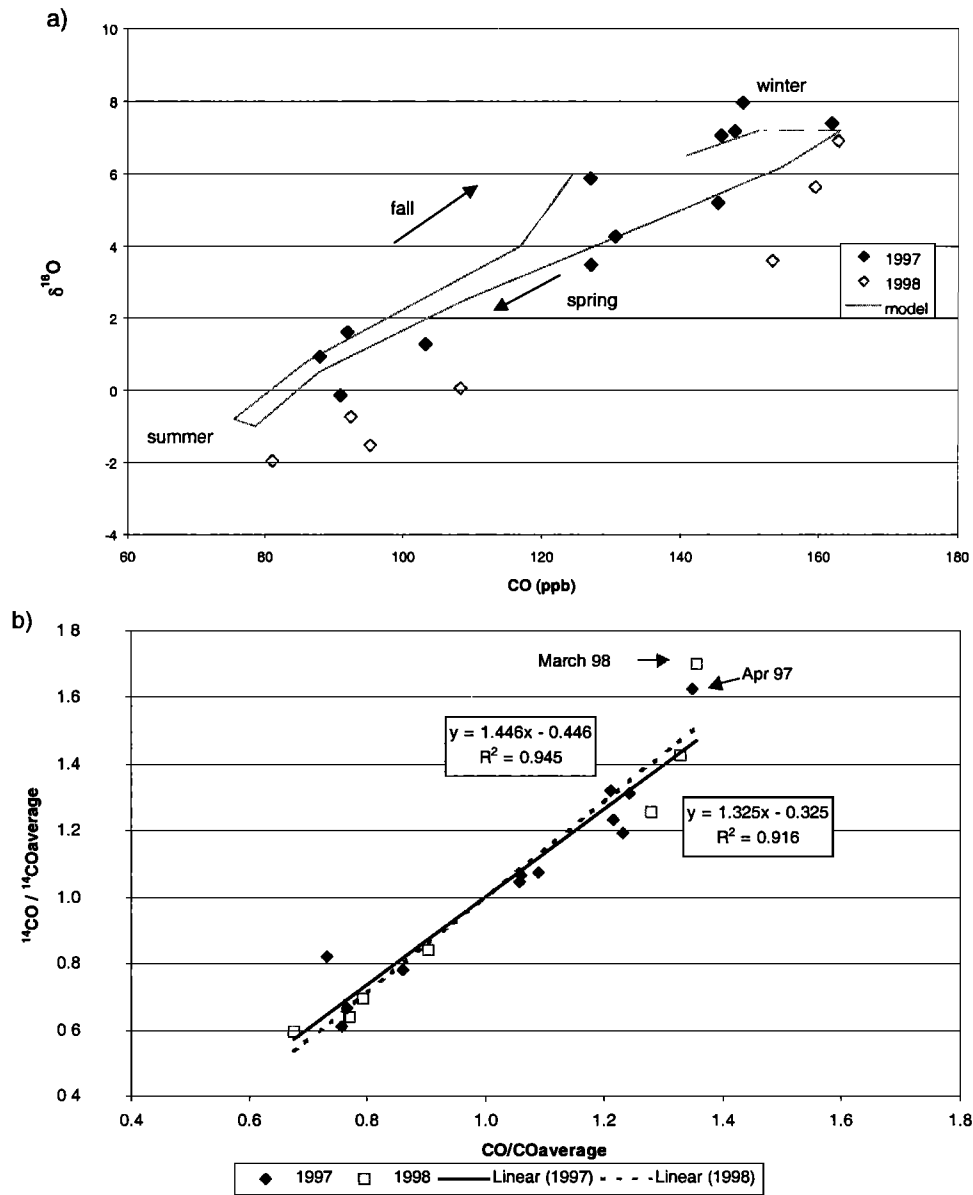


**Figure 4.** (a)  $\delta^{18}\text{O}$  and (b)  $^{14}\text{CO}$  plotted versus CO for 1997 and 1998. Most of the 1998 data were taken in spring and summer.

indicates that both seasonal cycles are mainly driven by the OH seasonality [Volz *et al.*, 1981]. However, the slopes of 1.3 and 1.4 observed for 1997 and 1998, respectively, show that  $^{14}\text{CO}$  seasonal gradients are considerably stronger. Therefore the sinks and sources have to be considered in more detail. The reaction rate in the main sink,  $\text{CO} + \text{OH}$ , is slightly lower for  $^{14}\text{CO}$ . If it is assumed that the fractionation for  $^{13}\text{CO}$  averaged over the pressure range of the troposphere is 3 ‰, the concomitant fractionation for  $^{14}\text{CO}$  is 6 ‰. Thus the rate of removal of  $^{14}\text{CO}$  is 0.6 % slower [Breninkmeijer *et al.*, 1999], and this cannot explain the large difference shown in Figure 4b. Concerning the source effect, for  $^{14}\text{CO}$  the import from the stratosphere peaks in spring, and this will indeed lead to a steeper slope in Figure 4b. The elevated  $^{14}\text{CO}$  levels observed in April 1997, and March 1998 may be indicative of this. There are also seasonal changes in CO sources. In summer the input of CO from the oxidation of methane and nonmethane hydrocarbons increases. This implies that during summer, the CO

inventory may not decline as rapidly as the  $^{14}\text{CO}$  inventory. The fact that when CO is produced from biogenic sources, also some  $^{14}\text{CO}$  is produced is of minor importance because of the low  $^{14}\text{C}$  content of biogenic CO compared to the atmospheric mix. Finally, we conclude that both CO and  $^{14}\text{CO}$  seasonal cycles are mainly driven by OH but that the CO minimum is partly offset by the increased summer sources.

There is little difference between the years 1997 and 1998 in Figure 4b. It is not expected that increased CO from biomass burning in the tropics, which is concluded from the  $\delta^{18}\text{O}$  data would affect the  $^{14}\text{CO}/\text{CO}$  relationship significantly. Another conclusion is that the stratosphere-troposphere exchange for the 2 years most likely has not been very different.

### 4.3. CO and $\delta^{18}\text{O}$ Outliers

As mentioned before, CO and  $\delta^{18}\text{O}$  were unexpectedly low for three samples in winter and spring, namely February 18, 1997,



**Table 2.** Results of CO and  $\delta^{18}\text{O}$  for the Three Outliers (See Text).

	CO		$\delta^{18}\text{O}$	
	Observed	Residual*	Observed	Residual*
Feb. 18, 1997	139 ppb	- 15 ppb	6.4 ‰	- 1.3 ‰
April 24, 1997	129 ppb	- 29 ppb	4.2 ‰	- 2.8 ‰
Feb. 2, 1998	130 ppb	- 26 ppb	4.5 ‰	- 2.5 ‰

\*Residual represents the difference between the observed value and the background value, as defined by the curve fitting.

and April 24, 1997, and February 2, 1998. The corresponding deviations from the background level are listed in Table 2. Coincident low values of CO and  $\delta^{18}\text{O}$  can have two origins: either transport from southern latitudes, or transport from the stratosphere. The last hypothesis is unlikely because observed  $^{14}\text{C}$  values are not elevated. To explain these events, we propose that air advected from southern latitudes was sampled, with low CO, low  $\delta^{18}\text{O}$  and low  $^{14}\text{C}$ . This hypothesis is consistent with  $\text{CH}_4$  results, which show relatively low values (1794 ppb, 1784 ppb, 1788 ppb) in agreement with the latitudinal gradient of this compound [Dlugokencky et al., 1994]. The air has then traveled through the upper troposphere and has reached higher latitudes, as confirmed by trajectories which show (for April 24, 1997 and February 2, 1998) that the air was at  $65^\circ\text{N}$ - $70^\circ\text{N}$  four days prior to the arrival at Sonnblick. The low RH of 30% associated with the three samples also is consistent with transport through the upper troposphere. Further, we conclude that the air mass has entrained some additional  $^{14}\text{C}$  at high altitude, the upper troposphere being enriched in  $^{14}\text{C}$  compared to the lower troposphere [Brenninkmeijer and Röckmann, 1997]. Other compounds having a significant positive vertical gradient in the troposphere, like  $^7\text{Be}$  or  $\text{O}_3$  [Zanis et al., 1999; WMO, 1999, and references therein] would also be enriched by such a mixing, which is confirmed by high  $^7\text{Be}$  for two of the three samples. The high variability of  $\text{O}_3$  does not allow one the use of this tracer for these events. Concerning CO, which has lower values in the upper troposphere than in the lower troposphere in the high latitudes of the Northern Hemisphere [Herman et al., 1999], the mixing of southern latitude air with polar upper tropospheric air would have kept CO at low levels.

## 5. Nonbackground Air

For the three categories of non-background air, namely, "subtropical," "polluted," and "stratospheric," we have calculated the corresponding "residual" values and all signatures for each

sample. The residual value is defined as the difference between the sample value and the corresponding background curve value. Table 3 gives the different results for CO and its isotopes along with results for  $^7\text{Be}$  and RH. Note that when repeated samples were taken within a short time, only the sample most characteristic of the event, that is, associated with the highest residual absolute value, was taken into account in the statistics. The results for the different categories will be discussed in the following sections. The absence of a  $\delta^{13}\text{C}$  specific signature can partly be attributed to its quite homogeneous distribution in the middle and high latitudes of the Northern Hemisphere. Indeed, the difference of the  $\delta^{13}\text{C}$  minimum and maximum annual levels observed between  $79^\circ\text{N}$  and  $28^\circ\text{N}$  are at most 2 ‰ to 3 ‰ (T. Röckmann et al., manuscript in preparation, 2000; M. Bräunlich et al., manuscript in preparation, 2000). Therefore the gradient observed between Sonnblick and other NH locations is at most 1 ‰ to 1.5 ‰.

### 5.1. Subtropical Air Masses

The observations of concurrent low CO, low  $\delta^{18}\text{O}$  and low  $^{14}\text{C}$  are most likely related to air mass transport from southern latitudes. The lower values of CO and  $\delta^{18}\text{O}$  reflect both the remoteness from the technological sources of CO (enriched in  $\text{C}^{18}\text{O}$ ) and the sink effect, the strength of which increases with decreasing latitude, following the OH latitudinal gradient. As mentioned above, lower  $^{14}\text{C}$  associated with lower latitudes is due to the combined effects of more OH and less cosmogenic  $^{14}\text{C}$ . We also note that during these events,  $\text{CH}_4$  and  $\text{SF}_6$  were significantly lower than the background level supporting a low latitude origin of the sampled air masses.

Sixteen samples (24% of the total) fall in this subtropical category and were taken between December and June. Table 3 summarizes the characteristics of the data belonging to this subtropical category. Compared to background levels, the results are lower by 32 ppb for CO, 3.5 ‰ for  $\delta^{18}\text{O}$  and 4.4 molecules  $\text{cm}^{-3}$

**Table 3.** Residuals, Representing the Deviation From the Background Signal, Calculated for CO,  $\delta^{18}\text{O}$ ,  $\delta^{13}\text{C}$ , and  $^{14}\text{C}$  for the Different Categories, Subtropical, Polluted and Stratospheric.

	Samples Quantity	CO, ppb	$\delta^{18}\text{O}$ , ‰	$\delta^{13}\text{C}$ , ‰	$^{14}\text{C}$ , molecule $\text{cm}^{-3}$	$^7\text{Be}$ , mBq $\text{m}^{-3}$	RH, %
Subtropical*	16	-34 (12)	-3.6 (2.0)	-0.3 (0.3)	-4.4 (1.9)	6.9 (3.0)	67 (23)
Subdivision 1	12	-42 (11)	-4.3 (1.8)	- 0.2 (0.3)	-5.2 (1.5)	7.5 (2.9)	57 (21)
Subdivision 2	4	-9 (2)	-1.4 (0.6)	- 0.5 (0.5)	-2.2 (0.8)	5.7 (3.3)	86 (14)
Polluted	12	+28 (11)	+2.9 (1.8)	+0.9 (1.7)	+1.4 (1.5)	5.0 (3.6)	91 (7)
Stratospheric	3	-16 (38)	-1.5 (2.7)	+0.3 (0.9)	+5.0 (1.9)	15.4 (10.3)	25 (9)

\*Subtropical data 1 and 2 represent the subdivisions described in text. Corresponding averages of  $^7\text{Be}$  and relative humidity (RH) are also given. Numbers in parentheses give the  $1\sigma$  standard deviation.

## SONNBLICK : Subtropical event

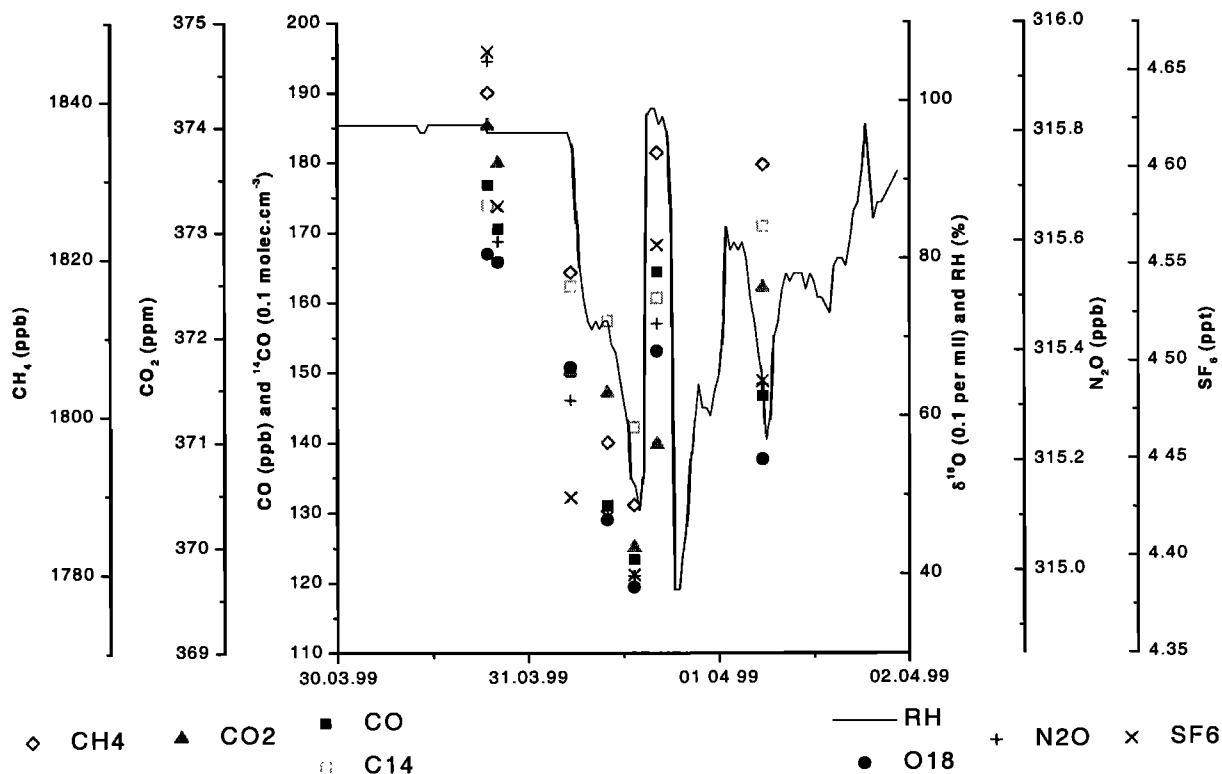


**Figure 5.** Subtropical air observed on March 31, 1999, with corresponding values of CO,  $^{14}\text{CO}$ ,  $\delta^{18}\text{O}$ ,  $\text{CH}_4$ ,  $\text{CO}_2$ ,  $\text{N}_2\text{O}$ ,  $\text{SF}_6$ , and relative humidity (RH).

for  $^{14}\text{CO}$ . However, there is a large scatter between the results, with the residual value of CO ranging from -6 to -60 ppb. Four samples were associated with relatively small residuals of -9 ppb for CO, -1.4 ‰ for  $\delta^{18}\text{O}$  and -2.2 molecules  $\text{cm}^{-3}$  for  $^{14}\text{CO}$  (subcategory 1 of Table 3). The high RH values (86% on average) associated with these four samples suggest that some air from the boundary layer has been injected during the transport, partly masking the original signature of the air mass (increase in CO and  $\text{C}^{18}\text{O}$ ). In contrast, a large part of the samples (subcategory 2 of Table 3) show large residuals of -42 ppb for CO, -4.3 ‰ for  $\delta^{18}\text{O}$  and -4.2 molecules  $\text{cm}^{-3}$  for  $^{14}\text{CO}$ . The low signatures in CO and isotopes of these data show that very clean air from low latitudes (south of  $30^\circ\text{N}$ ) was sampled.

Most of the corresponding back trajectories confirm that air masses are coming from latitudes south of  $35^\circ$ , mainly from the Atlantic Ocean and some from Africa. Note that  $^7\text{Be}$  and RH present medium values,  $6.9 \text{ mBq m}^{-3}$  and 67%, respectively, consistent with transport through the lower free troposphere, with little recent input from boundary layer air.

To better illustrate the events of very clean air from subtropical latitudes, we present in Figure 5 the results of repeated samples of March 30-31, 1999. CO and isotope results are given along with  $\text{CH}_4$ ,  $\text{CO}_2$ ,  $\text{N}_2\text{O}$ ,  $\text{SF}_6$ , and RH to trace the air mass origin. The first two samples (March 30, 1900 UTC and 2015 UTC) present 'normal' values of CO and  $\delta^{18}\text{O}$  and slightly low values of  $^{14}\text{CO}$ . These samples are associated with high RH, suggesting transport of air from the boundary layer. This would explain the relatively high CO and  $\delta^{18}\text{O}$  values compared to  $^{14}\text{CO}$  measurement, as this last compound is not affected by pollution (see next section).

At 400 UTC on March 31, RH suddenly drops, as do CO,  $\delta^{18}\text{O}$ ,  $^{14}\text{CO}$ , and other gases, indicating a change of the air mass origin. The lowest value of RH (48%) was reached at 1300 UTC, and the trace gas measurements also yielded minimum values. Compared to the first sample, the values have dropped by 54 ppb (CO), 4.2 ‰ ( $\delta^{18}\text{O}$ ), 3.2 molecules  $\text{cm}^{-3}$  ( $^{14}\text{CO}$ ), 52 ppb ( $\text{CH}_4$ ), 4 ppm ( $\text{CO}_2$ ), 0.9 ppb ( $\text{N}_2\text{O}$ ), and 0.26 ppt ( $\text{SF}_6$ ), suggesting that we are now sampling air from southern latitudes that had not been in contact with the boundary layer.

We compared these values with observations made during the same period (March 26, 1999) at Izaña ( $28^\circ\text{N}$ ) for CO and isotopes as well as for  $\text{CH}_4$ ,  $\text{CO}_2$ ,  $\text{N}_2\text{O}$  and  $\text{SF}_6$  (M. Bränlich, personal communication, 2000). The results from Izaña were 126 ppb (CO), 5 ‰ ( $\delta^{18}\text{O}$ ), 15.5 molecules  $\text{cm}^{-3}$  ( $^{14}\text{CO}$ ), 1799 ppb ( $\text{CH}_4$ ), 370.0 ppm ( $\text{CO}_2$ ), 4.42 ppt ( $\text{SF}_6$ ), and 314.8 ppb ( $\text{N}_2\text{O}$ ) which compare well with our observations of 123 ppb (CO), 3.8 ‰ ( $\delta^{18}\text{O}$ ), 14.2 molecules  $\text{cm}^{-3}$  ( $^{14}\text{CO}$ ), 1789 ppb ( $\text{CH}_4$ ), 370.0 ppm ( $\text{CO}_2$ ), 4.39 ppt ( $\text{SF}_6$ ), and 315.0 ppb ( $\text{N}_2\text{O}$ ) during this event. The good agreement between the two data sets suggests that the air sampled at Sonnblick has traveled from northern Africa with no significant mixing with other air masses. Obviously, even in a region dominated by zonal flows, meridional transport can take place, and the typical signature of an air mass from  $30^\circ\text{N}$  can be observed at  $50^\circ\text{N}$  some days later.

After the minimum observed at 1300 UTC, RH suddenly increases to a value of 100% within 1 hour. Samples taken at 1615 UTC reflect the last change in the air mass origin with values only slightly lower than those observed at the very beginning of the event. Note the considerable variability observed

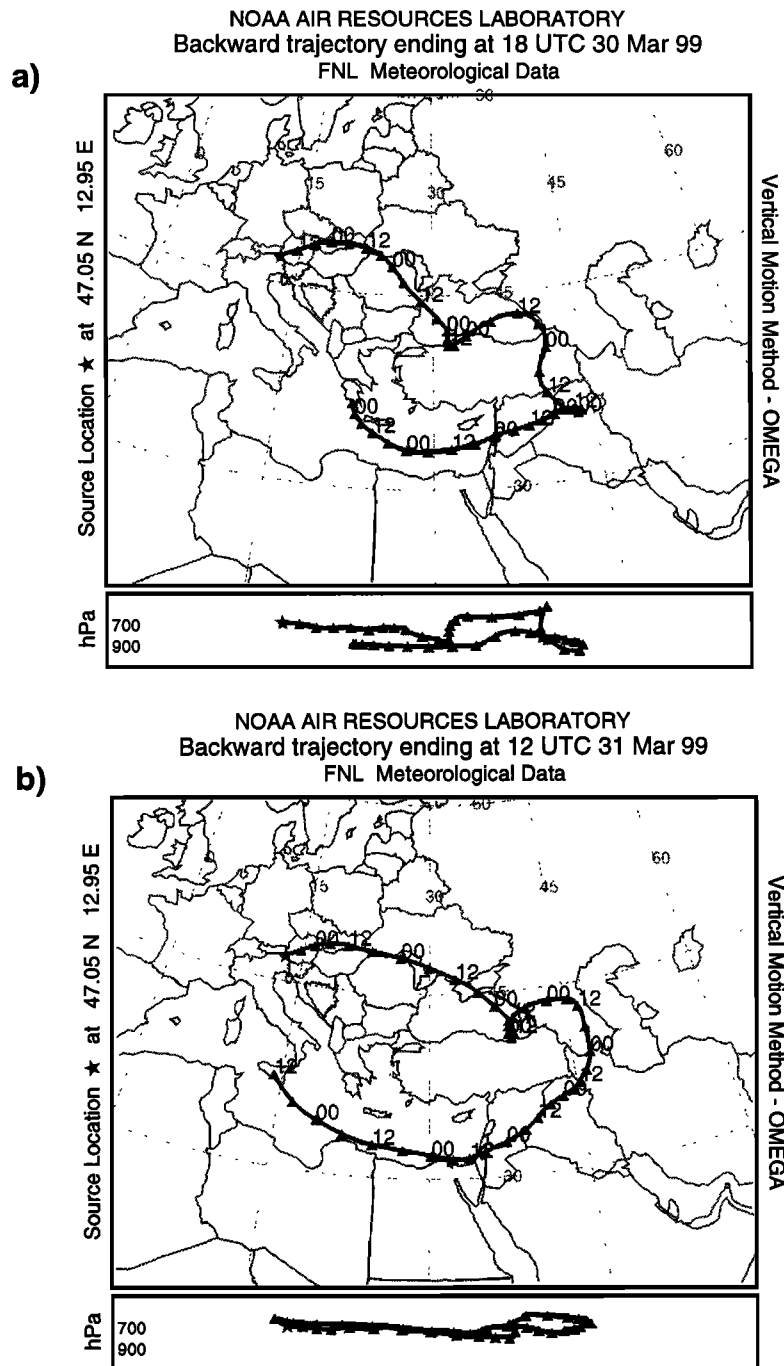


**Figure 6.** Ten-day backward trajectories for 1999: (a) March 30, 1800 UTC, (b) March 31, 1200 UTC, and (c) March 31, 1800 UTC. The trajectories were calculated with the Hybrid Single-Particle Lagrangian Integrated Trajectory (HYSPLIT4) model, 1997 (Web address: <http://www.arl.noaa.gov/ready/hysplit4.html>, NOAA Air Resources Laboratory, Silver Spring, Maryland).

on a very short timescale. Within 3 hours (with the RH change suggesting that it could be as short as 1 hour), CO increased by 41 ppb,  $\delta^{18}\text{O}$  increased by 3.0 ‰, and  $^{14}\text{CO}$  increased by 1.9 molecules  $\text{cm}^{-3}$ . Finally, the sample taken on April 1 presents intermediate values, similar to those observed on the morning of March 31.

The 10-day back trajectories corresponding to this event are presented in Figure 6 and confirm the features described above. On March 30, 1800 UTC (Figure 6a), transport from the south east with recent influence from the boundary layer is observed.

Then, on March 31, 1200 UTC (Figure 6b), the air comes from southern latitudes through the free troposphere, with the lowest latitude of 30°N reached 8 days before. Finally, on March 31, 1800 UTC (Figure 6c), air is originating from northwest.

From the measurements, meteorological data, and trajectory calculations, we conclude that Mt. Sonnblick was in a zone of transition between a flow of humid air in lower layers and a flow of relatively dry air from the east, with origin from southern latitudes, at higher levels. At the beginning, the lower flow was in contact with the ground with possible injections from the near-

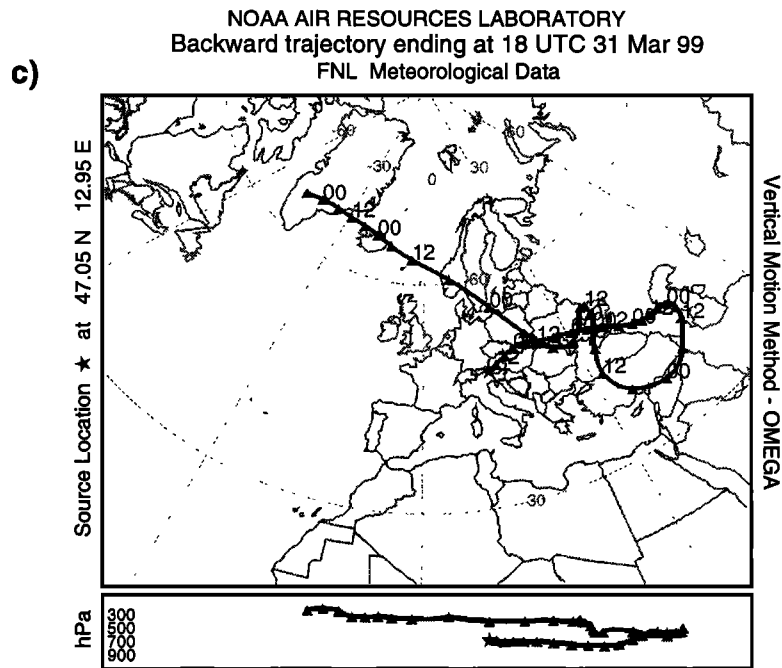


Figure 6. (continued)

ground emission sources, while later on there was no more contact with surface air. During the morning hours, when RH dropped to values near 50%, the flow in the upper layer originating from low latitudes had dominated at Sonnblick observatory, whereas during the afternoon, thermal convection must have caused updrift from the boundary layer. Finally during the evening, Sonnblick was no more influenced by boundary layer air.

### 5.2. Polluted Air Masses

Twelve samples (18% of the total) were affected by polluted air from the boundary layer. We identified these events based on their coincident high CO and  $\delta^{18}\text{O}$  results, with average residual values of +28 ppb for CO (with a minimum of +5 ppb and a maximum of +47 ppb) and +2.9 ‰ for  $\delta^{18}\text{O}$  (with extremes values of +0.01‰ and +6.8 ‰) (see Table 3). The high RH of 91% observed during these events is consistent with air originating from the boundary layer. The simultaneous enhancements of CO and  $\delta^{18}\text{O}$  are characteristic of the fossil fuel combustion source. This source, representing emissions from transportation, industries, and heating, is located at the surface and causes the strong gradient of CO between the boundary layer and the free troposphere observed over the continents [Roths and Harris, 1996]. It is important to note that  $^{14}\text{C}$ CO results are not affected by the combustion of fossil fuel pollution (residual of  $+1.4 \pm 1.5$  molecules  $\text{cm}^{-3}$ ) as expected from this source devoid of  $^{14}\text{C}$ .

Thus, although Sonnblick is generally located above the boundary layer, the observatory is not isolated from emissions occurring at the surface. Indeed, thermal convection and slope winds are known to bring air from the boundary layer to high elevation sites [Gäggeler et al., 1995; Baltensperger et al., 1997]. We note that half of the polluted events were observed in the summer months (July, August, and September) whereas no pollution events were found in winter months (January, February, and March). This seasonality reflects the degree of stability of the atmosphere, with greater vertical transport occurring in summer when the lower troposphere is less stable.

### 5.3. Stratospheric Air Masses

Carbon monoxide 14 constitutes a tracer of stratospheric air, as its mixing ratio is much higher in the stratosphere than in the troposphere [Brenninkmeijer et al., 1995; Jöckel et al. 1999]. We determined stratospheric influence at Sonnblick using this tracer, the threshold value being a residual value higher than +3 molecules  $\text{cm}^{-3}$ , in combination with the criteria defined by Stohl et al. [2000] for  $^7\text{Be}$ ,  $\text{O}_3$ , and RH. The corresponding thresholds were as follows: daily  $^7\text{Be}$  higher than 8  $\text{mBq m}^{-3}$ , daily minimum of RH lower than 30% and daily maximum of  $\text{O}_3$  at least 10% above the monthly mean. Samples fulfilling at least three of the criteria were selected as belonging to the stratospheric category.

Analysis of the data shows that only three samples (March 10, 1997, November 15, 1997, and August 7, 1998), representing 4% of the total number of samples, have been affected by stratospheric air. This frequency is lower than the one of 10% determined by Stohl et al. [2000] for Sonnblick; however, the difference is statistically not significant considering the small number of samples. Table 3 gives the characteristics of these data, which yield a positive residual value of +5.0 molecules  $\text{cm}^{-3}$  for  $^{14}\text{CO}$  and a mean value of 15.4  $\text{mBq m}^{-3}$  for  $^7\text{Be}$ . These data are associated with lower CO and lower  $\delta^{18}\text{O}$  than background values. This is in agreement with the study of Brenninkmeijer and Röckmann [1997] who found lower values of CO and  $\delta^{18}\text{O}$  for the stratosphere compared to the troposphere.

In November 1997 a sample was collected daily between the 15<sup>th</sup> and the 20<sup>th</sup>. The results for  $^{14}\text{CO}$ ,  $\text{O}_3$ , and  $^7\text{Be}$  are presented in Figure 7. Samples taken on November 14, 16, and 17 show no special feature and belong to the background category, with corresponding  $\text{O}_3$  levels ranging between 30 and 50 ppb. Air sampled on November 15 is associated with a  $^{14}\text{CO}$  value more than 20% higher than adjacent days, coincident with the maximum of a sharp  $\text{O}_3$  peak, showing a stratospheric influence. The corresponding CO and  $\delta^{18}\text{O}$  values are low, 110 ppb and 3.7‰ respectively, confirming that the  $\text{O}_3$  peak is not resulting from photochemical formation in polluted air. The daily average of  $^7\text{Be}$  is 8.6  $\text{Bq m}^{-3}$  while RH measurements are unavailable for this

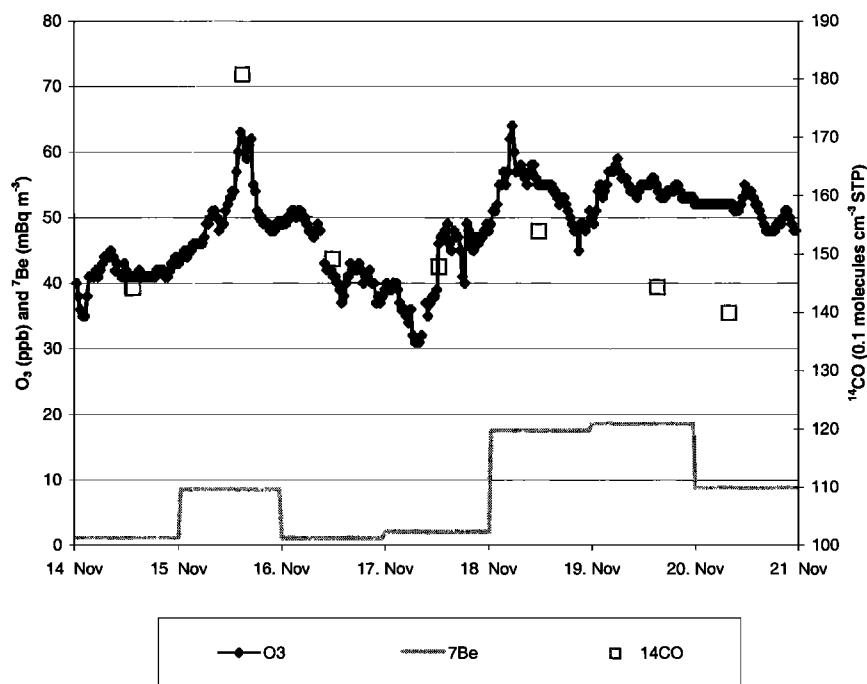


Figure 7. Stratospheric event of November 15, 1997, with corresponding data of  $^{14}\text{CO}$ ,  $\text{O}_3$ , and  $^7\text{Be}$ .

period. Finally, a study based on the calculations of 5-day back trajectories and corresponding potential vorticity (PV) was performed for this specific sampling date (H. Cuijpers, personal communication, 1999). It was found that about half of the 42 trajectories calculated inside a domain of  $5^\circ$  by  $5^\circ$  and 100 hPa around Sonnblick were associated with PV values higher than 1.5 PVU. This confirms that stratospheric air, originating from high latitudes, had reached Sonnblick on November 15. Additional evidence was obtained from the measurements ( $\text{O}_3$ ,  $^7\text{Be}$ , RH) at the Zugspitze, which showed a very pronounced stratospheric signature (E. Scheel, unpublished data, 2000).

For November 18 to 20, stratospheric episodes are characterized by  $\text{O}_3$  peaks coincident with high values of  $^7\text{Be}$  and low RH. However, the samples taken on these days did not coincide with the  $\text{O}_3$  daily maximum suggesting that these events were probably short-lived episodes. The absence of a significant increase of  $^{14}\text{CO}$  confirms that we did not see stratospheric influence on those samples.

In 1998, repeated samples were collected between August 7 and 10. A stratospheric event occurred on August 7 in the early morning when  $\text{O}_3$  peaked at 77 ppb (monthly mean: 53 ppb) and RH reached a minimum of 18% (Figure 8). The daily value of  $^7\text{Be}$  was exceptionally high at  $27.3 \text{ mBq m}^{-3}$ , reaching the highest value observed during the 3 years studied (September 1996 to August 1999). An air sample collected a couple of hours after this event contained high levels of  $^{14}\text{CO}$ , with a residual value of +6 molecules  $\text{cm}^{-3}$ . In contrast, CO and  $\delta^{18}\text{O}$ , which are expected to be low in stratospheric air, do show positive residual values of +27 ppb and +1.5 ‰, respectively. Since these residuals are calculated with respect to background levels, we can explain the discrepancy by a mixing of stratospheric air and polluted air from the troposphere, which might have occurred in the vicinity of Sonnblick. A previous study has shown that  $^{14}\text{CO}$  in the lowermost stratosphere of NH middle latitudes was about 60 molecules  $\text{cm}^{-3}$  [Zahn *et al.*, 2000]. A calculation shows that, with

a background level of 8 molecules  $\text{cm}^{-3}$  in the troposphere ( $^{14}\text{CO}$  is not affected by polluted air, see previous section) and a residual of +6 molecules  $\text{cm}^{-3}$ , 11 to 12% of the air was of stratospheric origin. If we assume a value of 60 ppb CO in the lowest stratosphere [Zahn *et al.*, 2000], the required value of CO in the troposphere to match the mixing would be about 130 ppb. Such a value, 40 ppb above the background level, can easily be observed in air recently affected by pollution of the boundary layer, as shown in the previous section. Such mixing of air masses would also explain the positive residual of  $\delta^{18}\text{O}$  observed during this event. The samples taken during August 7 reflect a simultaneous decrease of  $^{14}\text{CO}$  and  $\text{O}_3$  combined with an increase of RH. On August 8, and the following days, all parameters, except  $^7\text{Be}$  which is still high, show values representative of the background atmosphere. The characteristics of this stratospheric event were quite different from the one in November. Indeed, an analysis of the trajectories along with PV values did not indicate any recent stratospheric influence (H. Cuijpers, personal communication, 1999). However, due to the high intensity of this event, we can exclude stratospheric influence older than 5 days. We therefore suggest that this event reflects a strong stratospheric intrusion, probably too short to be captured by the trajectories and PV, which are based on 6-hour mean meteorological fields. This intrusion event was not very localised since a similar sharp stratospheric intrusion was also detected at the Zugspitze on the same day. Studies of atmospheric dynamics would be necessary to understand the mechanisms involved in this specific event.

## 6. Summary and Conclusions

Presented is an analysis of the first combined time series of CO,  $\delta^{18}\text{O}$ ,  $\delta^{13}\text{C}$ , and  $^{14}\text{CO}$  for a European continental station. The choice of Sonnblick station, Austrian Alps, was motivated by its location well above the boundary layer, allowing sampling of air not directly contaminated by the surrounding sources. However,

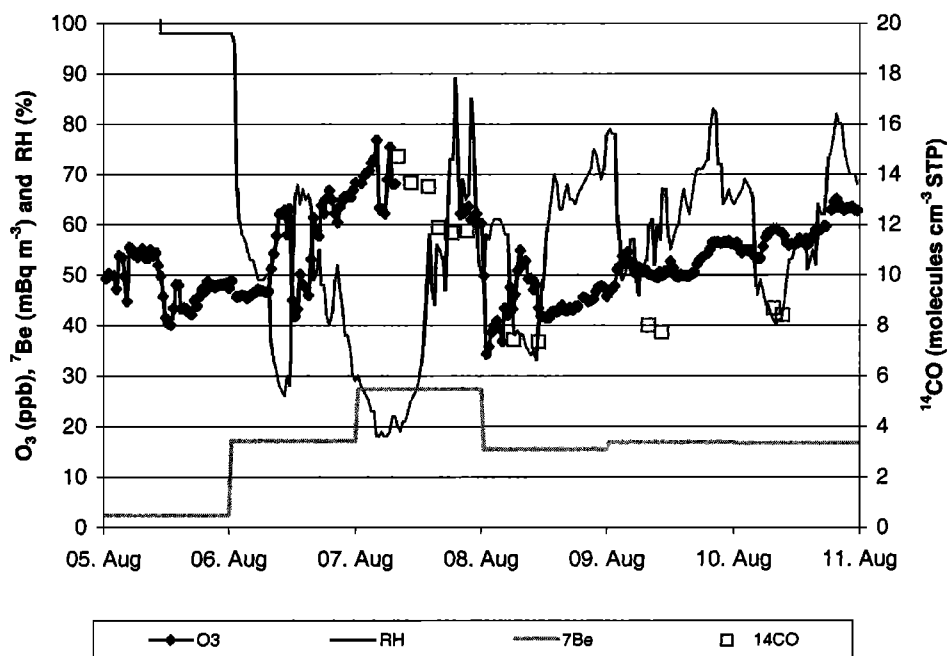


Figure 8. Stratospheric event of August 7, 1998, with corresponding data of  $^{14}\text{CO}$ ,  $\text{O}_3$ ,  $^7\text{Be}$ , and RH.

the high degree of variability observed in the results reflects wide variations in the origin of the air mass sampled. A detailed analysis of the data has allowed us to derive some characteristics of the air masses sampled.

The background data present well defined seasonal cycles with a minimum in summer and a maximum in late winter (shifted to spring for  $\delta^{13}\text{C}$ ). These seasonal variations are mainly driven by the OH sink of CO. There was no noticeable change in CO mixing ratios observed from 1997 to 1998, but the  $\delta^{18}\text{O}$  variation indicates that the origin of the CO observed has significantly changed between these 2 years. This variation is likely due to emissions of CO and its precursors from biomass burning.

Comparison of the observations of CO and stable isotopes with results of a global 3-D model has shown generally good agreement, supporting the CO,  $\delta^{13}\text{C}$  and  $\delta^{18}\text{O}$  source/sink distributions inferred by the model. According to the model results, the fossil fuel combustion source contributes 50% in winter and 35% in summer to the CO observed for this NH midlatitude area.

Most of the other samples were influenced by two different types of air, that is, clean air from the subtropics and polluted air of regional/continental origin. Characteristics associated with the subtropics data have shown that efficient transport over more than  $20^\circ$  latitude can take place with the original signature of the air mass being preserved. Concerning the polluted samples, lifting of air from the boundary layer, most efficiently by frontal systems, can result in transport of pollution from sources located at the ground. These three categories, background, subtropical, and polluted, establish the high degree of day-to-day variability observed at Sonnblick. A comparison with quasi-continuous CO measurements performed at Zugspitze have shown similar variability and a good agreement of the advection patterns. We conclude that the results obtained at Sonnblick for the isotopes are at least representative for the Alpine region.

We point out the importance of a classification of the air masses according to their origins. This is important in particular

for long-term studies when wanting to separate the impact of transport from the impact of sources and sinks. For instance, a higher frequency of subtropical air masses would otherwise lead to lower CO, lower  $\delta^{18}\text{O}$  and lower  $^{14}\text{CO}$  on average, but this would reflect a change in the circulation pattern and not a change in the sources/sinks of the compounds.

In addition to these categories, stratospheric influence has been indicated by three samples. Such an influence can have different origins, from long-range transport of products coming from the poleward stratosphere to stratospheric intrusions at shorter distances from the station, yielding high enhancement of the stratospheric tracers ( $^{14}\text{CO}$ ,  $\text{O}_3$ ,  $^7\text{Be}$ ).  $^{14}\text{CO}$  constitutes a powerful tracer, allowing one to determine the proportion of stratospheric air in an air mass, provided that background  $^{14}\text{CO}$ , derived for the NH midlatitudes in this paper, and  $^{14}\text{CO}$  levels in the stratosphere are known.

**Acknowledgments.** We would like to thank W. Hanewacker, C. Koepfel, and R. Hofmann for their careful analyses. The  $^7\text{Be}$  data were kindly provided by W. Ringer, Federal Institute for Food Control, Linz, Austria. The  $\text{O}_3$  data were provided by the Umweltbundesamt, and meteorological data were provided by the Central Institute for Meteorology and Geodynamics. We would like to thank P. Novelli for providing data from Hungary and for valuable discussions. We are grateful to A. Stohl for discussions concerning the criteria used for the definition of a stratospheric event and to H. Kromb-Kolb and P. Seibert for discussions about meteorology at Sonnblick. A special thanks to H. Cuijpers from Royal Netherlands Meteorological Institute (KNMI), who calculated and carefully analyzed the trajectories with PV values for the stratospheric events. Support from the European Community is gratefully acknowledged via the project CO-OH-Europe (ENV4-CT96-0318) and the Marie Curie Fellowship of V. Gros.

## References

- Appenzeller, C., J.R. Holton, and K.H. Rosenlof, Seasonal variation of mass transport across the tropopause, *J. Geophys. Res.*, *101*, 15,071-15,078, 1996.
- Baltensperger, U., H.W. Gäggeler, D.T. Jost, M. Lugauer, M. Schwikowski, E. Weingartner, and P. Seibert, Aerosol climatology at

- the high-alpine site Jungfraujoch, *J. Geophys. Res.*, *102*, 19,707-19,715, 1997.
- Bergamaschi, P., R. Hein, M. Heimann, and P.J. Crutzen, Inverse modeling of the global CO cycle, 1, Inversion of CO mixing ratios, *J. Geophys. Res.*, *105*, 1909-1927, 2000a.
- Bergamaschi, P., R. Hein, C.A.M. Brenninkmeijer, and P.J. Crutzen, Inverse modeling of the global CO cycle, 2, Inversion of  $^{13}\text{C}/^{12}\text{C}$  and  $^{18}\text{O}/^{16}\text{O}$  isotope ratios, *J. Geophys. Res.*, *105*, 1929-1945, 2000b.
- Bergamaschi, P., M. Bräunlich, T. Marik, and C.A.M. Brenninkmeijer, Measurements of the carbon and hydrogen isotopes of atmospheric methane at Izaña, Tenerife: Seasonal cycles and synoptic scale variations, *J. Geophys. Res.*, *105*, 14,531-14,546, 2000c.
- Bovensmann, H., J.P. Burrows, M. Buchwitz, J. Frerick, S. Noel, V.V. Rozanov, K.V. Chance, and A.P.H. Goede, SCIAMACHY: Mission objectives and measurement modes, *J. Atmos. Sci.*, *56*(2) 127-150, 1999.
- Brenninkmeijer, C.A.M., Measurement of the abundance of  $^{14}\text{C}$  in the atmosphere and the  $^{13}\text{C}/^{12}\text{C}$  and  $^{18}\text{O}/^{16}\text{O}$  ratio of atmospheric CO with applications in New Zealand and Antarctica, *J. Geophys. Res.*, *98*, 10,595-10,614, 1993.
- Brenninkmeijer, C.A.M., M.R. Manning, D.C. Lowe, J. Sparks, G. Wallace, and A. Volz-Thomas, Interhemispheric asymmetry in OH abundance inferred from measurements of atmospheric  $^{14}\text{C}$ , *Nature*, *356*, 50-54, 1992.
- Brenninkmeijer, C.A.M., D.C. Lowe, M.R. Manning, R. J. Sparks, and P.F.J. van Velthoven, The  $^{13}\text{C}$ ,  $^{14}\text{C}$ , and  $^{18}\text{O}$  isotopic composition of CO, CH<sub>4</sub>, and CO<sub>2</sub> in the higher southern latitudes lower stratosphere, *J. Geophys. Res.*, *100*, 26,163-26,172, 1995.
- Brenninkmeijer, C.A.M., and T. Röckmann, Principal factors determining the  $^{18}\text{O}/^{16}\text{O}$  ratio of atmospheric CO as derived from observations in the southern hemispheric troposphere and lowermost stratosphere, *J. Geophys. Res.*, *102*, 25,477-25,485, 1997.
- Brenninkmeijer, C.A.M., T. Röckmann, M. Bräunlich, P. Jöckel, and P. Bergamaschi, Review of progress in isotopes studies of atmospheric carbon monoxide, *Chemosphere Global Change Sc.*, *1*, 33-52, 1999.
- Brenninkmeijer, C.A.M., C. Koepfel, T. Röckmann, D.S. Scharffe, M. Bräunlich, and V. Gros, Absolute measurement of the abundance of atmospheric carbon monoxide, *J. Geophys. Res.*, in press, 2000.
- Cantrell, C.A., R.E. Shetter, A.H. McDaniel, J.G. Calvert, J.A. Davidson, D.C. Lowe, S.C. Tyler, R.J. Cicerone, and J.P. Greenberg, Carbon kinetic isotope effect in the oxidation of methane by the hydroxyl radical, *J. Geophys. Res.*, *95*, 22,455-22,462, 1990.
- Conny, J.M., The isotopic characterization of carbon monoxide in the troposphere, *Atmos Environ.*, *32*, 2669-2683, 1998.
- Conny, J.M., R.M. Verkouteren, and L.A. Currie, Carbon 13 composition of tropospheric CO in Brazil: A model scenario during the biomass burning season, *J. Geophys. Res.*, *102*, 10,683-10,693, 1997.
- Cooke, W.F., B. Koffi, and J.M. Gregoire, Seasonality of vegetation fires in Africa from remote sensing data and application to a global chemistry model, *J. Geophys. Res.*, *101*, 21,051-21,065, 1996.
- Derwent, R.G., P.G. Simmonds, S. Seuring, and C. Dimmer, Observation and interpretation of the seasonal cycles in the surface concentrations of ozone and carbon monoxide at Mace Head, Ireland from 1990 to 1994, *Atmos Environ.*, *32*, 145-157, 1998.
- Dlugokencky, E.J., L.P. Steele, P.M. Lang, and K.A. Masarie, The growth rate and distribution of atmospheric methane, *J. Geophys. Res.*, *99*, 17,021-17,043, 1994.
- Draxler, R.R., and G.D. Hess, Description of the Hysplit\_4 modeling system, *NOAA Tech. Memo. ERL ARL-224*, 24 pp., Natl. Oceanic and Atmos. Admin., Silver Spring, Md., 1997.
- Edwards, D.P., C.M. Halvorson, and J.C. Gille, Radiative transfer modeling for the EOS Terra satellite Measurement of Pollution in the Troposphere (MOPITT) instrument, *J. Geophys. Res.*, *104*, 16,755-16,775, 1999.
- Fay, B., H. Glaab, I. Jacobsen, and R. Schrodin, Evaluation of Eulerian and Lagrangian Atmospheric Transport Models at the Deutscher Wetterdienst using Anatex Surface Tracer Data, *Atmos. Environ.*, *18*, 2485-2497, 1995.
- Gäggeler, H.W., D.T. Jost, U. Baltensperger, M. Schwikowski, and P. Seibert, Radon and Thoron decay product and  $^{210}\text{Pb}$  measurements at Jungfraujoch, Switzerland, *Atmos. Environ.*, *29*, 607-616, 1995.
- Herman, R.L., et al., Measurements of CO in the upper troposphere and lower stratosphere, *Chemosphere Global Change Sc.*, *1*, 173-183, 1999.
- Huff, A.K., and M.H. Thiemens,  $^{17}\text{O}/^{16}\text{O}$  and  $^{18}\text{O}/^{16}\text{O}$  isotopes measurements of atmospheric carbon monoxide and its sources, *Geophys. Res. Lett.*, *25*, 3509-3512, 1998.
- Intergovernmental Panel on Climate Change (IPCC), *Climate Change 1994: Radiative Forcing of Climate Change and an Evaluation of the IPCC IS 92 Emissions Scenarios*, edited by J.T. Houghton et al., 339 pp., Cambridge Univ. Press, New York, 1995.
- Jöckel, P., Cosmogenic  $^{14}\text{C}$  as tracer for atmospheric chemistry and transport, PhD-Thesis, Combined Faculties for the Natural Sciences and for Mathematics, Rupertus Carola University, Heidelberg, Germany, 2000.
- Jöckel, P., M.G. Lawrence, and C.A.M. Brenninkmeijer, Simulations of cosmogenic  $^{14}\text{C}$  using the three-dimensional atmospheric model MATCH: Effects of  $^{14}\text{C}$  production and the solar cycle, *J. Geophys. Res.*, *104*, 11,733-11,743, 1999.
- Jöckel, P., C.A.M. Brenninkmeijer, and M.G. Lawrence, Atmospheric response time of cosmogenic  $^{14}\text{C}$  to changes in solar activity, *J. Geophys. Res.*, *105*, 6737-6744, 2000.
- Kato, S., H. Akimoto, M. Bräunlich, T. Röckmann, and C.A.M. Brenninkmeijer, Measurements of stable carbon and oxygen isotopic compositions of CO in automobile exhausts and ambient air from semi-urban Mainz, Germany, *Geochem. J.*, *33*, 73-77, 1999.
- Kato, S., K. Yoshizumi, H. Akimoto, M. Bräunlich, T. Röckmann, and C.A.M. Brenninkmeijer, Observed and modeled seasonal variation of  $^{13}\text{C}$ ,  $^{18}\text{O}$ , and  $^{14}\text{C}$  of atmospheric CO at Happo, a remote site in Japan, and a comparison with other records, *J. Geophys. Res.*, *105*, 8891-8900, 2000.
- Krol, M., P.J. van Leeuwen, and J. Lelieveld, Global OH trend inferred from methylchloroform measurements, *J. Geophys. Res.*, *103*, 10,697-10,711, 1998.
- Levine, J.S., The 1997 fires in Kalimantan and Sumatra, Indonesia: Gaseous and particulate emissions, *Geophys. Res. Lett.*, *26*, 815-818, 1999.
- Lingenfelter, R.E., Production of carbon 14 by cosmic-ray neutrons, *Rev. Geophys.*, *1*, 35-55, 1963.
- MacKay, C., M. Pandow, and R. Wolfgang, On the chemistry of natural radiocarbon, *J. Geophys. Res.*, *68*, 3929-3931, 1963.
- Maiss, M., and C.A.M. Brenninkmeijer, Atmospheric SF<sub>6</sub>: Trends, sources and prospects, *Environ. Sci. Technol.*, *32*, 3077-3086, 1998.
- Maiss, M., P. Steele, R. Francey, P. Fraser, R. Langenfelds, N.B.A. Trivett, and I. Levin, Sulfur hexafluoride - A powerful new atmospheric tracer, *Atmos. Environ.*, *30*, 1621-1629, 1996.
- Mak, J.E., and C.A.M. Brenninkmeijer, Compressed air sample technology for isotopic analysis of atmospheric carbon monoxide, *J. Atmos. Oceanic Technol.*, *11*, 425-431, 1994.
- Mak, J.E., and G. Kra, The isotopic composition of carbon monoxide at Montauk Point, Long Island, *Chemosphere Global Change Sc.*, *1*, 205-218, 1999.
- Mak, J.E., and J.R. Southon, Assessment of tropical OH seasonality using atmospheric  $^{14}\text{C}$  measurements from Barbados, *Geophys. Res. Lett.*, *25*, 2801-2804, 1998.
- Novelli, P.C., K.A. Masarie, and P.M. Lang, Distributions and recent changes in tropospheric CO, *J. Geophys. Res.*, *103*, 19,015-19,033, 1998.
- Pandow, M., C. MacKay, and R. Wolfgang, The reaction of atomic carbon with oxygen: Significance for the natural radio-carbon cycle, *J. Inorg. Nucl. Chem.*, *14*, 153-158, 1960.
- Quay, P.D., et al., Carbon isotopic composition of atmospheric CH<sub>4</sub>: Fossil and biomass burning source strength, *Global Biogeochem. Cycles*, *5*, 25-47, 1991.
- Röckmann, T., Measurement and interpretation of  $^{13}\text{C}$ ,  $^{14}\text{C}$ ,  $^{17}\text{O}$  and  $^{18}\text{O}$  variations in atmospheric carbon monoxide, PhD Thesis, 151 pp., Univ. of Heidelberg, Heidelberg, Germany, 1998.
- Röckmann, T., C.A.M. Brenninkmeijer, G. Saueressig, P. Bergamaschi, J. Crowley, H. Fischer, and P.J. Crutzen, Mass independent fractionation of oxygen isotopes in atmospheric CO due to the reaction CO + OH, *Science*, *281*, 544-546, 1998.
- Rom, W., C.A.M. Brenninkmeijer, C.B. Ramsey, W. Kutschera, A. Priller, S. Puchegger, T. Röckmann and P. Steier, Methodological aspects of atmospheric  $^{14}\text{C}$  measurements with AMS, *Nucl. Instrum. Meth. B*, in press, 2000a.
- Rom, W. et al., A detailed 2-year record of atmospheric  $^{14}\text{C}$  in the temperate northern hemisphere, *Nucl. Instrum. Meth. B*, *161*, 780-785, 2000b.
- Roths, J., and G.W. Harris, The tropospheric distribution of carbon monoxide as observed during the TROPOZ II experiment, *J. Atmos. Chem.*, *24*, 157-188, 1996.
- Scheel, H.E., E.-G. Brunke, R. Sladkovic, and W. Seiler, In situ CO concentrations at the sites Zugspitze (47°N, 11°E) and Cape Point

- (34°S, 18°E) in April and October 1994, *J. Geophys. Res.*, *103*, 19,295-19,304, 1998.
- Seibert, P. H. Kromp-Kolb, A. Kasper, M. Kalina, H. Puxbaum, D.T. Jost, M. Schwikowski, and U. Baltensperger, Transport of polluted boundary layer air from the Po Valley to high-alpine sites, *Atmos. Environ.*, *32*, 3953-3965, 1998.
- Smit, H.G.J., A. Volz, D.H. Ehhalt, and H. Knappe, The isotopic fractionation during the oxidation of carbon monoxide by hydroxyl radicals and its implications for the atmospheric CO-cycle, in *Stable Isotopes*, edited by H.-L. Schmidt, H. Förstel, and K. Heinziger, pp. 147-152, Elsevier Sci., New York, 1982.
- Stevens, C.M., and A.F. Wagner, The role of isotope fractionation effects in atmospheric chemistry, *Z. Naturforsch.*, *44A*, 376-384, 1989.
- Stevens, C.M., L. Krout, D. Walling, A. Venters, A. Engelkemeir, and L.E. Ross, The isotopic composition of atmospheric carbon monoxide, *Earth Planet. Sci. Lett.*, *16*, 147-165, 1972.
- Stohl, A., N. Spichtinger-Rakowsky, P. Bonasoni, H. Feldmann, M. Memmesheimer, H.E. Scheel, T. Trickl, S. Hübener, W. Ringer, and M. Mandl, The influence of stratospheric intrusions on alpine ozone concentrations, *Atmos. Environ.*, *34*, 1323-1354, 2000.
- Tyler, S.C., G.A. Klouda, G.W. Brailsford, A.C. Manning, J.M. Conny, and A.J. Timothy Jull, Seasonal snapshots of the isotopic (<sup>14</sup>C, <sup>13</sup>C) composition of tropospheric carbon monoxide at Niwot Ridge, Colorado, *Chemosphere Global Change Sc.*, *1*, 185-203, 1999.
- Volz, A., D.H. Ehhalt, and R.G. Derwent, Seasonal and latitudinal variation of <sup>14</sup>CO and the tropospheric concentration of OH radicals, *J. Geophys. Res.*, *86*, 5163-5171, 1981.
- World Meteorological Organization (WMO), Scientific assessment of ozone depletion: 1998, *Rep. 44*, Global Ozone Res. and Monit. Proj., Geneva, 1999.
- Zahn, A., et al., Identification of extratropical two-way troposphere-stratosphere mixing based on CARIBIC measurements of O<sub>3</sub>, CO, and ultrafine particles, *J. Geophys. Res.*, *105*, 1527-1535, 2000.
- Zanis, P., E. Schuepbach, H.W. Gäggeler, S. Hübener, and L. Tobler, Factors controlling beryllium-7 at Jungfraujoch, *Tellus, Ser. B.*, *51*, 789-805, 1999.
- 
- P. Bergamaschi, Höllentalstr. 94, D-79199 Kirchzarten, Germany.  
M. Bräunlich, C.A.M. Brenninkmeijer, V. Gros, P. Jöckel, and T. Röckmann, Air Chemistry Division, Max Planck Institute for Chemistry, Mainz D-55020, Germany. (vgros@mpch-mainz.mpg.de)  
A. Kaiser, Central Institute for Meteorology and Geodynamics, A-1190, Vienna, Austria.  
W. Kustchera, Vienna Environmental Research Accelerator, Institute for Isotope Research and Nuclear Physics, University of Vienna, A-1090 Vienna, Austria.  
M. Mandl, Central Institute for Meteorology and Geodynamics, A-5020, Salzburg, Austria  
G. Possnert, Ångström Laboratory, University of Uppsala, S-751 21 Uppsala, Sweden.  
W. Rom, AMS <sup>14</sup>C Dating Laboratory, Ny Munkegade, DK-8000 Aarhus, Denmark.  
H. E. Scheel, Fraunhofer Institute, D-82467 Garmisch-Partenkirchen, Germany.  
J. van der Plicht, Centre for Isotope Research, University of Groningen, NL-9747 Groningen, Netherlands

(Received June 12, 2000; revised August 8, 2000; accepted August 14, 2000.)